Dendritic cells in the tumor microenvironment: prognostic and theranostic impact

Johanna Verneau, Catherine Sautés-Fridman, Cheng-Ming Sun

Investigation of the effect of water content on the mechanical behavior of track-bed materials under various coarse grain contents

Yu Su, Yu-Jun Cui, Jean-Claude Dupla, Jean Canou

Laboratoire Navier/CERMES, Ecole des Ponts ParisTech (ENPC), France

Corresponding author

Professor Yu-Jun Cui

Ecole des Ponts ParisTech, Laboratoire Navier/CERMES, 6 – 8 av. Blaise Pascal, Cité Descartes, Champs-sur-Marne, 77455 Marne – la – Vallée cedex 2, France

Tel.: +33 164153550

Fax: +33 164153562

E-mail address: yu-jun.cui@enpc.fr

Abstract

In the French conventional railway track, an interlayer was created naturally through the interpenetration of ballast and subgrade under the effect of long-term train loading. Field investigation showed that the proportion of ballast grains decreased over depth in the interlayer. Moreover, the water content of interlayer soils varied depending on the weather conditions, which can strongly affect the mechanical behavior of interlayer soil. In this study, the effect of water content on the mechanical behavior of interlayer soils under various coarse grain contents was investigated by monotonic triaxial tests. Three water contents (w = 17.6%, 10.6%, and 7.0%), five volumetric coarse grain contents (f_v = 0%, 10%, 20%, 35%, and 45%) and three confining pressures (σ_3 = 30, 60 and 120 kPa) were considered. Results showed that a decrease of w led to an increase of shear strength and soil stiffness due to the effect of suction, and to an increase of dilatancy due to the aggregation of fine soils. Moreover, the variations of maximum deviator stress q_{max}, Young's modulus E_0, dilatancy angle ψ and friction angle φ with f_v followed a bi-linear pattern for the three σ_3 values, defining a characteristic volumetric coarse grain content $f_{v\text{-}cha}$ value for a given w value: $f_{v\text{-}cha} \approx$ 25%, 29% and 33% for w = 17.6%, 10.6% and 7.0%, respectively. The $f_{v\text{-}cha}$ corresponded to the transition from a structure dominated by fine soils to a structure dominated by coarse grains. The increase of $f_{v\text{-}cha}$ with the decrease of w could be attributed to the swelling and shrinkage of fines. While drying from optimum water content of fines $w_{opt\text{-}f}$ =13.7% to a lower w_f value, more coarse grains were needed to constitute the global skeleton due to the increase of the global volume of macro-pores resulted from the shrinkage of fine soils. By contrast, while wetting from $w_{opt\text{-}f}$ =13.7% to a higher w_f value, since the global volume of macro-pores

43 decreased due to the swelling of fine soils, less coarse grains were required to constitute the
44 global skeleton.

45 **Keywords:** fabric/structure of soils; partial saturation; laboratory tests; compaction; shear
46 strength

47 INTRODUCTION

48 Most French conventional railway track was constructed by putting the ballast layer on the
49 subgrade soil directly. Due to the long-term train circulation, a layer namely interlayer was
50 naturally formed in the substructure, mainly by the interpenetration of ballast and subgrade.
51 Considering its high dry density (2.4 Mg /m^3) and high bearing capacity [1], the French
52 railway company (SNCF) has decided to keep it as part of the substructure in the execution of
53 the track renewal program [2].

54 Based on the field investigation, the content of ballast grains was found to decrease over
55 depth [1]. Globally, the interlayer can be separated into two parts: the upper part dominated by
56 ballast grains and the lower part dominated by fine soils. For the upper part, the effects of fine
57 soil content and water content on the mechanical behavior were studied by Trinh et al. [3],
58 Cui et al. [2], Duong et al. [4-6] and Lamas-Lopez et al. [7, 8] by performing monotonic and
59 cyclic triaxial tests. In order to extend the study to the whole interlayer, Wang et al. [9-11] and
60 Qi et al. [12] investigated the effect of coarse grain content f_v (volumetric ratio of coarse
61 grains to total sample) on the mechanical behavior. Results revealed existence of a
62 characteristic volumetric coarse grain content $f_{v\text{-}cha}$, below which the soil was characterised by
63 a fine matrix with coarse grains floating in it, while beyond which the soil was characterised
64 by a coarse grain skeleton. It is worth noting that in the previous studies, the effect of f_v on the
65 mechanical behavior was investigated under constant water content conditions. This is
66 obviously not the field condition where the water content varies depending on the weather
67 conditions, resulting in changes in mechanical behavior. Therefore, from a practical point of

68 view, it appears essential to investigate the effect of water content on the mechanical behavior
69 of interlayer soil.

70 There are several studies addressing the effect of coarse grain content on the mechanical
71 behavior of soil. Seif El Dine et al. [13] worked on sandy matrix with f_v of gravels, showing
72 an increase of shear strength with the increase of f_v. However, Vallejo [14] showed an
73 opposite trend when the mass proportion of coarse particles was beyond 65% for a mixture of
74 rock and sand. It is worth noting that the fines involved in their studies were cohesionless soils
75 like sand and glass beads, which did not represent the natural fine soils in the interlayer. Wang
76 et al. [9-11] studied the effect of f_v on the static and dynamic responses of interlayer soil, and
77 identified a characteristic value $f_{v\text{-}cha}$ that could be used to differentiate two distinct soil fabrics.
78 Qi et al. [12] investigated the effect of the coefficient of uniformity C_u of coarse grains on the
79 mechanical behavior of interlayer soils, and found that the decrease of C_u led to an increase of
80 $f_{v\text{-}cha}$. A few studies were undertaken to investigate the water content effect on the mechanical
81 behavior of substructure soils in terms of shear strength, resilient modulus, etc. Trinh et al. [3]
82 investigated the effect of water content on the mechanical behavior of fouled ballast at
83 different water contents and found that the lower the water content, the higher the shear
84 strength. Duong et al. [6] studied the effect of water content on the resilient modulus of the
85 upper part interlayer soil by large-scale cyclic triaxial tests, and reported that the increase of
86 water content gave rise to a decrease of resilient modulus. To the author's knowledge, there
87 has been no work addressing the effect of water content on $f_{v\text{-}cha}$.

88 In this study, the effect of water content on the mechanical behavior of the interlayer soil
89 at various f_v values was investigated by performing monotonic triaxial tests under different

90 confining pressures. Three water contents (17.6%, 10.6%, and 7.0%), five coarse grain
91 contents (0%, 10%, 20%, 35%, and 45%) and three confining pressures (30, 60 and 120 kPa)
92 were considered. The mechanical properties including Young's modulus E_0, Poisson's ratio v,
93 dilatancy angle ψ, friction angle φ and cohesion c were analyzed. The results obtained allowed
94 the effect of water content on the characteristic volumetric coarse grain content $f_{v\text{-}cha}$ to be
95 clarified.
96
97 MATERIALS AND METHODS
98 *Materials and sample preparation*
99 Since it was difficult to obtain intact interlayer soil, the studied soil was reconstituted in the
100 laboratory. For the fines, in order to simulate the grain size distribution of fine soils from
101 'Senissiat site' (Fig. 1), nine different commercial soils including sand and clay were mixed,
102 with the pre-determined proportions shown in Table 1. The liquid limit and plasticity index of
103 the reconstituted fine soil were 32% and 20%, respectively defining the fine soil as CL
104 according to the universal soil classification system (Fig. 2). A good agreement between real
105 fine soil and reconstituted fine soil was observed in terms of grain size distribution (Fig. 1),
106 liquid limit and plasticity index (Fig. 2). Standard Proctor compaction was performed
107 following ASTM D698-12 [15] for the reconstituted fine soil (Fig. 3), allowing an optimum
108 water content $w_{opt\text{-}f}$ = 13.7% and a maximum dry density $\rho_{dmax\text{-}f}$ = 1.82 Mg/m^3 to be identified.

109 For the coarse grains, following the parallel similitude method adopted by Wang et al. [10]
110 and Qi et al. [12], micro-ballast was prepared to represent the real ballast by using three
111 granular materials G 4-10, HN 2-4 and G 10-20, as shown in Fig. 4. In order to quantify the

112 amount of micro-ballast in a sample, a parameter namely volumetric coarse grain content f_v
113 [9-13] was adopted:

114 $$f_v = V_{in} / V_{total} \quad (1)$$

115 where V_{in} and V_{total} represent the coarse grain volume and the total sample volume,
116 respectively. Note that the total sample volume V_{total} was composed of the coarse grain volume
117 V_{in} and the fine soil volume V_{fines}. The dry density of fine soil in all samples was controlled at
118 $\rho_{dmax\text{-}f}$ = 1.82 Mg/m^3 (Table 2). At a given f_v value, the dry mass of coarse grain, the dry mass
119 of fine soil and the water content contained in the fine soil can be calculated. Details about the
120 calculation could be found in Wang et al. [10].

121 For the preparation of samples at target f_v and w_f, the fine soil was prepared at optimum
122 water content $w_{opt\text{-}f}$ = 13.7%, then stored in a container for 24 h for moisture homogenization.
123 The fine soil was then mixed with micro-ballast grains thoroughly to reach the target f_v value.
124 In order to attain a satisfactory homogeneity of the soil mixture, it was dynamically
125 compacted in three layers, with the equivalent amount of fine soil and micro-ballast for each
126 layer, to reach a total size of 100 mm diameter and 200 mm height. Fig.5 shows the samples
127 with various f_v values, compacted at $w_{opt\text{-}f}$ = 13.7%. Note that at a given compaction effort, the
128 dry density of fine soil changes with the variation of coarse grain content f_v. Since the dry
129 density of fine soil in all samples was controlled at $\rho_{dmax\text{-}f}$ = 1.82 Mg/m^3, the compaction
130 efforts was higher for the samples at higher f_v values. As a result, higher ρ_d values were
131 obtained for the samples with higher f_v values, as shown in Table 2.

132 After reaching the target f_v value, either a wetting or a drying process was adopted to
133 obtain the target w_f: w_1 = 17.6% on the wet side of optimum; w_2 = 10.6% and w_3 = 7.0% on the
134 dry side of optimum. In the case of drying process, considering that a too fast drying would
135 lead to sample damage by fissuring, a milder drying method was performed: the sample was
136 exposed to the air in the laboratory for 1 h each time, and then wrapped with plastic film for
137 equilibration. The time of equilibration needed was determined by measurement of suction
138 and water content in three positions: in the center, ½ r and r, with r being radius of the sample.
139 The results obtained showed that 7 h was required for reaching reasonable equilibration in
140 terms of suction and water content (Table 3). In the case of wetting process, 10 g water was
141 sprayed on the sample each time prior to covering it with plastic film for equilibration. The
142 same equilibration time of at least 7 h was adopted.

143 When wetting or drying to a target w_f, the volume of sample was measured by means of a
144 caliper. The volume changes from initial water content $w_{opt\text{-}f}$ = 13.7% to different target w_f
145 values are presented in Fig. 6. It appears that at a given f_v value, an increase of water content
146 from $w_{opt\text{-}f}$ = 13.7% to w_1= 17.6% led to sample swelling, while a decrease of water content
147 from $w_{opt\text{-}f}$ = 13.7% to w_2= 10.6% or w_3= 7.0% led to sample shrinkage. Moreover, under a
148 given water content, the sample exhibited lower swelling-shrinkage with higher f_v values,
149 illustrating the sensitivity of fine soil to water content changes. The measured dry densities of
150 samples after wetting or drying are shown in Table 2.

151

152 *Monotonic triaxial tests*

153 The monotonic triaxial apparatus shown in Fig. 7 was adopted in this study. The mechanical
154 behavior of soil at five different f_v values (0%, 10%, 20%, 35%, and 45%) and three different
155 w_f contents (17.6%, 10.6%, and 7.0%) was investigated by monotonic triaxial tests, under
156 three different σ_3 values (30, 60 and 120 kPa). These confining pressures σ_3 were determined
157 by the consideration of wheel load of train, the depth of interlayer soil from 250 mm to 600
158 mm and the Poisson ratio of 0.3-0.4 proposed by Selig and Waters [16]. Considering the
159 wheel load of 16-22 tons per axle in France and 30 tons per axle of heavier train in other
160 countries [17], the corresponding range of vertical stress was estimated at 40 - 90 kPa and 120
161 - 140 kPa [4], respectively ; the average horizontal stress was estimated at 30 kPa and 60 kPa,
162 respectively. In this study, the maximum horizontal stress 120 kPa was adopted, which was
163 the same to that adopted by Wang et al. [10]. Note that all samples were prepared to reach the
164 target water contents (w_1 = 17.6% on the wet side, or w_2 = 10.6% and w_3 = 7.0% on the dry
165 side) prior to starting the test. For the samples at w_1 = 17.6% (S_r = 100%), an overnight
166 consolidation under the corresponding confining pressure was adopted prior to shearing, to
167 ensure the dissipation of pore water pressure. On the contrary, for the samples at w_2 = 10.6%
168 (S_r = 60%) or w_3 = 7.0% (S_r = 40%), after an application of σ_3, the sample was directly sheared,
169 because only air was expected to be expelled. A shear rate as low as 0.1mm/min was adopted
170 for all tests. The tests ended when a peak deviator stress appeared or the axial strain ε_1 reached
171 15% in case without occurrence of peak deviator stress.

172

173 EXPERIMENTAL RESULTS

174 *Variation of shear behavior with f_v*

175 The variations of deviator stress q and volumetric strain ε_v with axial strain ε_1 for samples at
176 w_1 = 17.6% and five different f_v values are depicted in Fig. 8. It can be observed from Figs.
177 8a$_1$-8a$_3$ that under a given confining pressure σ_3 value, the maximum deviator stress q_{max}
178 increased slowly with the increase of f_v for $f_v \leq 20\%$, while the increase of q_{max} was more
179 pronounced for $f_v \geq 35\%$. The similar phenomena can be observed for the case of w_2 = 10.6%
180 and w_3 = 7.0%.

181 In Fig. 8b$_1$, pure contractancy behaviour was observed for samples at $f_v \leq 20\%$, while for
182 samples at $f_v \geq 35\%$, a behavior of contractancy followed by dilatancy was identified.
183 Moreover, the larger the f_v value, the more pronounced the dilatancy behaviour. This dilatancy
184 was however reduced by the increase of confining pressure: when σ_3 was increased from 60
185 kPa (Fig. 8b$_2$) to 120 kPa (Fig. 8b$_3$), the contractancy increased and the dilatancy decreased.

186

187 *Variation of maximum deviator stress q_{max} with w*

188 Fig. 9 depicts the variations of q_{max} against f_v at different σ_3 values for three different water
189 contents. In the case of w_1 = 17.6% (Fig. 9a), it appears that under a given σ_3 value, the
190 variation of q_{max} followed a bi-linear pattern with two different slopes, which defined a
191 characteristic volumetric coarse grain content $f_{v\text{-}cha}$. Moreover, similar $f_{v\text{-}cha}$ values (around
192 25%) could be identified for the three different σ_3 values. Physically, the $f_{v\text{-}cha}$ value
193 distinguished two different soil fabrics: when $f_v \leq f_{v\text{-}cha}$, the soil fabric was governed by fine

194 soil dominated structure, while when $f_v \geq f_{v\text{-}cha}$ it was governed by coarse grain dominated
195 structure, in agreement with the observations by Wang et al. [10] and Qi et al. [12].

196 The same phenomena were observed for the two other water contents: $w_2 = 10.6\%$ (Fig.
197 9b) and $w_3 = 7.0\%$ (Fig. 9c). For each water content, q_{max} varies in a bi-linear fashion with
198 with f_v, defining a $f_{v\text{-}cha}$ value which is independent of the σ_3 value. The values of $f_{v\text{-}cha}$ were 29%
199 and 33% for $w_2 = 10.6\%$ and $w_3 = 7.0\%$, respectively. Comparison of the $f_{v\text{-}cha}$ values at
200 different water contents showed that $f_{v\text{-}cha}$ increased with the decrease of water content.

201

202 *Variation of Young's modulus E_0 with w*

203 In this study, the Young's modulus E_0, was defined as the ratio of deviator stress to axial
204 strain from 0% to 1%. Fig. 10 shows the variations of E_0 with f_v under different σ_3 values for
205 the three water contents. The effect of w on Young's modulus E_0 can be clearly observed: at a
206 given f_v and σ_3, E_0 increased with the decrease of water content. This was attributed to the
207 increase of suction with the decrease of water content. At a given water content, a bi-linear
208 fitting could be also applied to represent changes of E_0 with f_v for all σ_3 values. This also
209 defined a characteristic volumetric coarse grain content $f_{v\text{-}cha}$, which was independent of σ_3. As
210 far as the variation of $f_{v\text{-}cha}$ with w was concerned, it appeared from Fig. 10 that $f_{v\text{-}cha}$ increased
211 with the decrease of w: $f_{v\text{-}cha}$ was around 25% for $w_1 = 17.6\%$ (Fig. 10a), 29% for $w_2 = 10.6\%$
212 (Fig. 10b) and 33% for $w_3 = 7\%$ (Fig. 10c), which agreed well with the previous observation
213 while studying the effect of water content on q_{max} in Fig. 9.

214

Variations of Poisson's ratio v and dilatancy angle ψ with w

Based on the volumetric strain-axial strain curves, the Poisson's ratio v and the dilatancy angle ψ were determined using respectively Eqs. (1) and (2) [18]:

$$v = (1- k_c)/2 \quad (1)$$

$$\sin \psi = k_D /(-2+ k_D) \quad (2)$$

where k_c and k_D are the slopes of volumetric strain-axial strain curves in the contractancy phase and dilatancy phase, respectively.

Fig. 11 depicts the variations of Poisson's ratio v versus f_v at different σ_3 values for three water contents. At $w_1 = 17.6\%$ (Fig. 11a), v was not significantly influenced by σ_3 and f_v, with the values fluctuating around $v = 0.36$. The values of v at $f_v \leq 20\%$ were slightly larger than those at $f_v \geq 35\%$. This was due to the transition of soil fabric from fine soils dominated structure to coarse grains dominated structure, which resulted in the increase of soil stiffness and the decrease of horizontal strain. Moreover, the difference of v between $f_v \leq 20\%$ and $f_v \geq 35\%$ decreased with the decrease of water content. The average value of v was 0.21 at $w_2 = 10.6\%$ (Fig. 11b) and 0.19 at $w_3 = 7.0\%$ (Fig. 11c). At $w_3 = 7.0\%$, the v remained almost unchanged with the increase of f_v. Overall, it appeares that the average value of v decreased with the decreasing water content, suggesting that the lateral strain was reduced by the increase of suction or decrease of water content.

The effect of w on the dilatancy angle ψ can be clearly observed in Fig. 12: under given f_v and σ_3 values, the ψ increased with the decrease of w. This could be attributed to the

235 aggregation of fine soil induced by the increase of suction. Indeed, a lower water content
236 would generate a higher suction. In that case, the fine soils behaved more like granular
237 materials, exhibiting more dilatancy behavior, as shown by Cui and Delage [19] and Ng et al.
238 [20].

239 As shown in Fig. 12a (w_1 = 17.6%), no dilatancy behavior was observed for f_v varying
240 from 0% to 20% at all σ_3 values, whereas an obvious dilatancy behaviour was observed for f_v =
241 35% at σ_3 = 30 kPa and for f_v = 45% at all σ_3 values. In addition, in Fig. 12b and Fig. 12c, a
242 distinct change of ψ was observed from $f_v \leq 20\%$ to $f_v \geq 35\%$, defining a value of characteristic
243 volumetric coarse grain content $f_{v\text{-}cha} \approx 29\%$ at w_2 = 10.6% and $f_{v\text{-}cha} \approx 33\%$ at w_3 = 7.0%. This
244 increase of $f_{v\text{-}cha}$ with the decrease of water content was consistent with the observation of
245 water effect on q_{max} and E_0.

246

247 *Variations of cohesion c and friction angle φ with w*

248 The values of cohesion c and friction angle φ were determined based on the peak deviator
249 stress values. Fig.13 depicts the variation of cohesion c with w. It can be observed that at a
250 given f_v, the cohesion c increased with the decrease of water content. This could be attributed
251 to the effect of suction on the fine soil.

252 For the friction angle φ, Fig.14 shows that φ increased with the decrease of w. This
253 confirmed the aggregation phenomenon with the decrease of w for the fine soils. The similar
254 observation was made by Zhao et al. [21] while studying the shear strength of a mixture of
255 sand, silt and gravel. Moreover, under a given w, a bi-linear pattern of increasing trend with f_v

was observed for φ. A value of $f_{v\text{-}cha}$ could be thus identified for each water content: $f_{v\text{-}cha} \approx$ 25%, 29%, 33% for w = 17.6%, 10.6%, 7.0%, respectively, in agreement with the effects of water content on q_{max}, E_0 and ψ.

DISCUSSIONS

The test results showed that the value of $f_{v\text{-}cha}$ increased with the decrease of water content, as shown in Table 4. Wang et al. [10] obtained a value of $f_{v\text{-}cha}$ equal to 27% at the optimum water content $w_{opt\text{-}f}$ = 13.7%, which came to confirm the observation made in this study.

As mentioned before, the $f_{v\text{-}cha}$ corresponded to the transition of soil fabric: when $f_v \leq f_{v\text{-}cha}$, the soil fabric was the fine soil dominated structure, while when $f_v \geq f_{v\text{-}cha}$, the soil fabric changed to the coarse grains dominated structure. In other words, the $f_{v\text{-}cha}$ represented the minimum f_v value needed for forming a coarse grains dominated structure. When $f_v \geq f_{v\text{-}cha}$, two categories of fine soil were expected, namely a first category of dense fine soil situated between coarse grains and a second category of loose fine soil situated in the macro-pores surrounded by coarse grains. The former contributed to the loading-bearing skeleton of coarse grains, whereas the latter contributed little, as concluded by de Frias Lopez [22] through discrete element analysis.

The variation of $f_{v\text{-}cha}$ with w could be attributed to the swelling upon wetting and shrinkage upon drying of these two categories of fines. With the decrease of water content, the two categories of fine soil would shrink. The shrinkage of the first category of fines would lead to a decrease of macro-pores between coarse grains, while the shrinkage of the second

277 category would lead to an increase of macro-pores surrounded by coarse grains. As the
278 density was expected to be higher and the quantity was expected to be smaller for the first
279 category of fines, the decrease of macro-pores volume due to the shrinkage of the first
280 category of fines was expected to be much smaller than the increase of macro-pores volume
281 due to the shrinkage of the second category of fines. This was supported by the observation
282 from Zhang and Li [23] using mercury intrusion porosimetry, who studied the fine/coarse soil
283 mixture and reported that the structure supported by coarse grains was stable, and thus the
284 shrinkage of clayey soils gave rise to an increase of the volume of macro-pores surrounded by
285 coarse particles. The effect of shrinkage of fine soil was also observed by Fies et al. [24] for
286 the ternary mixtures of sand, silt and clay soils. They reported that when the fine fraction
287 contained larger than 25% clay content, the shrinkage of fine fraction gave rise to the
288 formation of macro-pores among the coarse fraction. It is worth noting that in this study, 30%
289 of clay content of Speswhite and Bentonite were shown in Table 1 for the fine fraction, which
290 contributed to the formation of macro-pores in the coarse grain skeleton. Thus, with the
291 increase of volume of macro-pores, more coarse grains were needed to constitute a global
292 skeleton. This is characterized by the increase of $f_{v\text{-}cha}$ value.
293
294 CONCLUSIONS
295 The effect of w on the mechanical behavior of interlayer soil at various f_v was investigated by
296 monotonic triaxial tests. Three water contents (w = 17.6%, 10.6%, and 7.0%), five volumetric
297 coarse grain contents (f_v = 0%, 10%, 20%, 35% and 45%) and three confining pressures (σ_3 =

298 30, 60 and 120 kPa) were considered. The obtained results allowed the following conclusions
299 to be drawn.

300 The decrease of water content led to an increase of the peak deviator stress q_{max} and the
301 Young's modulus E_0. This could be explained by the effect of suction with the decrease of
302 water content. The Poisson's ratio v was found to decrease with the decrease of water content,
303 because the horizontal deformation was reduced by the increase of suction. The dilatancy
304 angle ψ and the friction angle φ were found to increase with the decrease of water content.
305 This was attributed to the aggregation of fine soil induced by the increase of suction,
306 enhancing the dilatancy behavior and the friction of soil. A larger cohesion c was observed at
307 lower w, also due to the effect of suction in fine soil.

308 The variation of q_{max}, E_0, ψ, and φ with f_v followed a bi-linear pattern, defining a same
309 characteristic $f_{v\text{-}cha}$ value for a given w value: $f_{v\text{-}cha} \approx 25\%$, 29% and 33% for w = 17.6%, 10.6%
310 and 7.0%, respectively. The value of $f_{v\text{-}cha} \approx 27\%$ at w_{opt} = 13.7% reported by Wang et al.
311 (2018a) came to support this observation. This was attributed to the swelling upon wetting and
312 shrinkage upon drying of two categories of fine soil: a first category of dense fine soil situated
313 between coarse grains and a second category of loose fine soil situated in the macro-pores
314 surrounded by coarse grains. With the decrease of water content, the two categories of fine
315 soils would shrink. Moreover, the shrinkage of the first category of fines would lead to a
316 decrease of macro-pores between coarse grains, while the shrinkage of the second category
317 would lead to an increase of macro-pores surrounded by coarse grains. As the decrease of
318 macro-pores volume due to the shrinkage of the first category of fines was expected to be

much smaller than the increase of macro-pores volume due to the shrinkage of the second category of fines, the global macro-pores volume was increasing with the decrease of water content. In that case, more coarse grains were needed to constitute a global skeleton, leading to an increase of $f_{v\text{-}cha}$.

ACKNOWLEDGEMENTS

This work was supported by the Chinese Scholar Council (CSC) and Ecole des Ponts ParisTech.

REFERENCES

[1] V. N. Trinh, Comportement hydromécanique des matériaux constitutifs de plateformes ferroviaires anciennes. PhD Thesis, Ecole Nationale des Ponts et Chaussées, Université Paris-Est, 2011.

[2] Y.J. Cui, T.V. Duong, A.M. Tang, J.C. Dupla, N. Calon, A. Robinet, Investigation of the hydro-mechanical behaviour of fouled ballast, Journal of Zhejiang University Science A. 14(4) (2013) 244-255.

[3] V.N. Trinh, A.M. Tang, Y.J. Cui, J.C. Dupla, J. Canou, N. Calon, L. Lambert, A. Robinet, O. Schoen, Mechanical characterisation of the fouled ballast in ancient railway track substructure by large-scale triaxial tests, Soils and foundations. 52(3) (2012) 511-523.

338 [4] T.V. Duong, A.M. Tang, Y.J. Cui, V.N. Trinh, J.C. Dupla, N. Calon, J. Canou, A. Robinet,
339 Effects of fines and water contents on the mechanical behavior of interlayer soil in
340 ancient railway sub-structure, Soils and foundations. 53(6) (2013) 868-878.
341 [5] T.V. Duong, Y.J. Cui, A.M. Tang, J.C. Dupla, J. Canou, N. Calon, A. Robinet,
342 Investigating the mud pumping and interlayer creation phenomena in railway sub-
343 structure, Engineering geology. 171 (2014) 45-58.
344 [6] T.V. Duong, Y.J. Cui, A.M. Tang, J.C. Dupla, J. Canou, N. Calon, A. Robinet, Effects of
345 water and fines contents on the resilient modulus of the interlayer soil of railway
346 substructure, Acta Geotechnica. 11(1) (2016) 51-59.
347 [7] F. Lamas-Lopez, S.C. d'Aguiar, A. Robinet, Y.J. Cui, N. Calon, J. Canou, J.C. Dupla,
348 A.M. Tang, In-situ investigation of the behaviour of a French conventional railway
349 platform, In Proceedings of the transportation research board 94th annual meeting.
350 Washington, DC (2015) 15-1076.
351 [8] F. Lamas-lopez, Field and laboratory investigation on the dynamic behavior of
352 conventional railway track-bed materials in the context of traffic upgrade. PhD Thesis,
353 Ecole Nationale des Ponts et Chaussées, Université Paris-Est, 2016.
354 [9] H.L. Wang, Y.J. Cui, F. Lamas-Lopez, J.C. Dupla, J. Canou, N. Calon, G. Saussine, P.
355 Aimedieu, R.P. Chen, Effects of inclusion contents on resilient modulus and damping
356 ratio of unsaturated track-bed materials, Canadian Geotechnical Journal. 54 (12) (2017)
357 1672-1681.
358 [10] H.L. Wang, Y.J. Cui, F. Lamas-Lopez, N. Calon, G. Saussine, J.C. Dupla, J. Canou, P.
359 Aimedieu, R.P. Chen, Investigation on the mechanical behavior of track-bed materials at

various contents of coarse grains, Construction and Building Materials. 164 (2018) 228-237.

[11] H.L. Wang, Y.J. Cui, F. Lamas-Lopez, J.C. Dupla, J. Canou, N. Calon, G. Saussine, P. Aimedieu, R.P. Chen, Permanent deformation of track-bed materials at various inclusion contents under large number of loading cycles, Journal of Geotechnical and Geoenvironmental Engineering. 144(8) (2018) 04018044.

[12] S. Qi, Y.J. Cui, R.P. Chen, H.L. Wang, F. Lamas-Lopez, P. Aimedieu, J.C. Dupla, J. Canou, G. Saussine, Influence of grain size distribution of inclusions on the mechanical behaviours of track-bed materials, Géotechnique. (2019) 1-10.

[13] B. Seif El Dine, J. C. Dupla, R. Frank, J. Canou, Y. Kazan, Mechanical characterization of matrix coarse-grained soils with a large-sized triaxial device, Canadian Geotechnical Journal. 47(4) (2010) 425-438.

[14] L.E. Vallejo, Interpretation of the limits in shear strength in binary granular mixtures, Canadian Geotechnical Journal. 38(5) (2001) 1097-1104.

[15] ASTM D698-12. Standard test methods for laboratory compaction characteristics of soil using standard effort. ASTM International, West Conshohocken, Pa, 2012.

[16] E.T. Selig, J.M. Waters, Track geotechnology and substructure management. Thomas Telford, 1994.

[17] J. Alias, La voie ferrée. Techniques de construction et d'entretien, 2nd Ed., Eyrolles, 1984.

[18] P.A. Vermeer, R. De Borst, Non-associated plasticity for soils, concrete and rock. HERON, 29(3) (1984) 1-64.

382 [19] Y.J. Cui, P. Delage, Yeilding and plastic behaviour of an unsaturated compacted silt,
383 Géotechnique. 46(2) (1996) 291-311.
384 [20] C.W.W. Ng, S. Baghbanrezvan, H. Sadeghi, C. Zhou, F. Jafarzadeh, Effect of specimen
385 preparation techniques on dynamic properties of unsaturated fine-grained soil at high
386 suctions, Canadian Geotechnical Journal. 54(9) (2017) 1310-1319.
387 [21] H.F. Zhao, L.M. Zhang, D.G. Fredlund, Bimodal shear-strength behavior of unsaturated
388 coarse-grained soils, Journal of geotechnical and geoenvironmental engineering. 139(12)
389 (2013) 2070-2081.
390 [22] R. de Frias Lopez, J. Silfwerbrand, D. Jelagin, B. Birgisson, Force transmission and soil
391 fabric of binary granular mixtures, Géotechnique. 66(7) (2016)578-583.
392 [23] L.M. Zhang, X. Li, Microporosity structure of coarse granular soils, Journal of
393 Geotechnical and Geoenvironmental Engineering. 136(10) (2010)1425-1436.
394 [24] J.C. Fiès, N.D.E., Louvigny, A. Chanzy The role of stones in soil water retention,
395 European Journal of Soil Science. 53(1) (2002) 95-104.

396 NOTATIONS

c	cohesion
E_0	initial Young's modulus
f_v	volumetric coarse grain content
$f_{v\text{-}cha}$	characteristic volumetric coarse grain content
k_c	slope of volume change curve in the contractancy phase
k_D	slope of volume change curve in the dilatancy phase
ρ_d	dry density of sample
$\rho_{dmax\text{-}f}$	maximum dry density of fine soil
q	deviator stress
q_{max}	peak deviator stress
$w_{opt\text{-}f}$	optimum water content of fine soil
w_f	water content of fine soil
ε_a	axial strain
ε_v	volumetric strain
σ_3	confining pressure
φ	friction angle
v	Poisson's ratio
ψ	dilatancy angle

397

398

399 LIST OF TABLES

400

401 LIST OF FIGURES

402

403

404 Table 1. The constitution of fine soil

Soil	Mass proportion (%)	Grain size range (mm)
HN34	3.3	0.063 - 0.50
HN31	3.3	0.16 - 0.63
HN0.4-0.8	6.7	0.25 - 1
HN0.6-1.6	6.7	0.32 - 2
HN1-2.5	13.3	0.32 – 3.20
C4	16.7	0.0009 – 0.50
C10	20	0.0009 – 0.25
Speswhite	23.3	0.0003 – 0.01
Bentonite	6.7	0.001 – 0.01

405

406

407 Table 2. Experimental program

f_v (%)	Initial water content w_{opt-f} (%)	Target w_f (%)	Target S_r (%)	Target ρ_{dmax-f} (Mg/m^3)	Target ρ_d (Mg/m^3)	Measured ρ_d (Mg/m^3)	Confining pressure σ_3 (kPa)		
0	13.7	17.6	100	1.82	1.82	1.80	30	60	120
		10.6	60			1.85	30	60	120
		7.0	40			1.86	30	60	120
10		17.6	100		1.91	1.88	30	60	120
		10.6	60			1.93	30	60	120
		7.0	40			1.94	30	60	120
20		17.6	100		1.99	1.97	30	60	120
		10.6	60			2.01	30	60	120
		7.0	40			2.03	30	60	120
35		17.6	100		2.12	2.11	30	60	120
		10.6	60			2.13	30	60	120
		7.0	40			2.13	30	60	120
45		17.6	100		2.21	2.20	30	60	120
		10.6	60			2.22	30	60	120
		7.0	40			2.23	30	60	120

Note: f_v represents the ratio of volumetric inclusion content to the total volume of the sample [10]. w_{opt-f}, w_f, S_r and ρ_{dmax-f} represent the optimum water content, the water content, the degree of saturation and the maximum dry density of fine soils, respectively. ρ_d represents the dry density of soil mixture sample. Measured ρ_d represents the dry density of soil mixture sample after wetting or drying from compaction water content w_{opt-f} to target w_f.

Table 3. Suction and water content measured at different equilibration times for fine soils

Position	Suction (MPa)	Water content (%)	Suction (MPa)	Water content (%)
	After 6h		After 7h	
center	0.33	12.7	0.32	12.9
1/2 r	0.24	13.5	0.35	12.8
r	0.46	13.7	0.33	13.1

Table 4. $f_{v\text{-}cha}$ values at different water contents

w (%)	17.6	13.7	10.6	7.0
$f_{v\text{-}cha}$ (%)	25	27	29	33

Note: $f_{v\text{-}cha} \approx 27\%$ corresponding to $w = 13.7\%$ was obtained by Wang et al. [10]

408

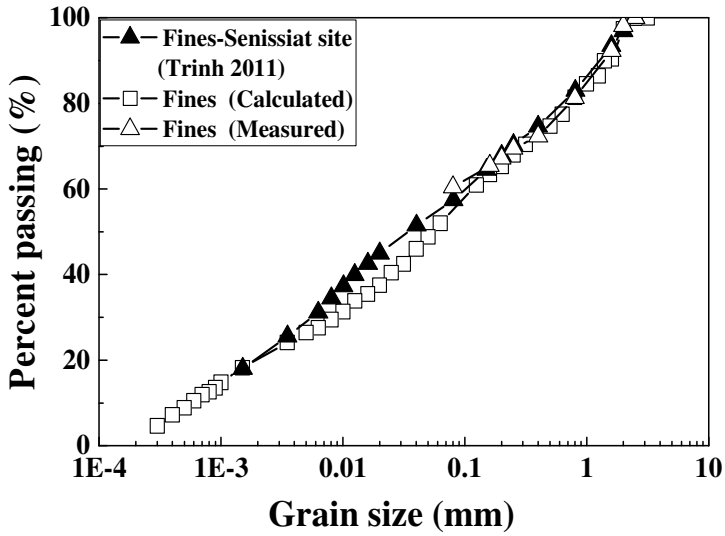

409

Fig. 1. Grain size distribution curves of fine soils (after Wang et al. [10])

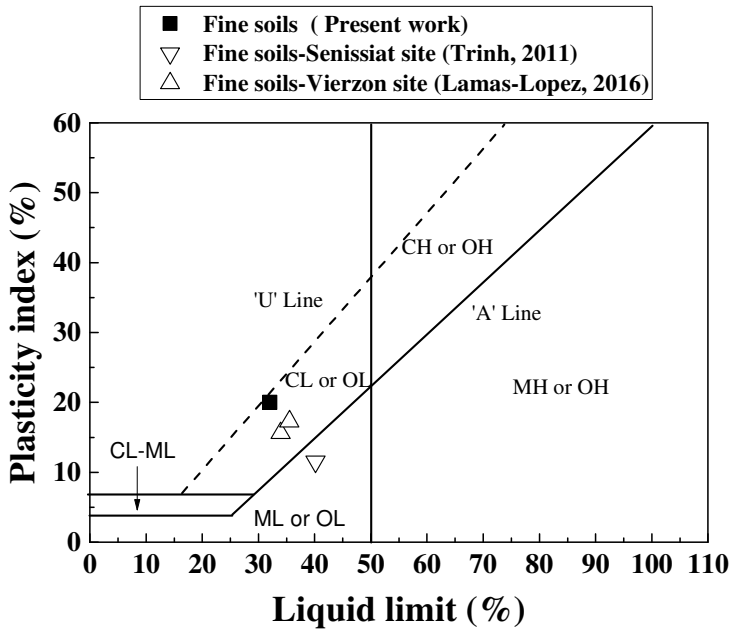

410

Fig. 2. Plasticity of fine soils (after Wang et al. [10])

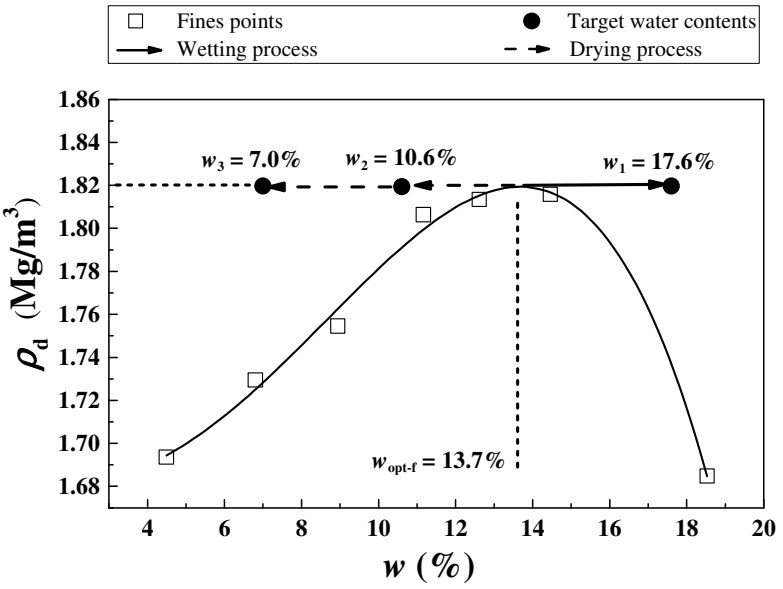

Fig. 3. Samples states with respect to the compaction curve

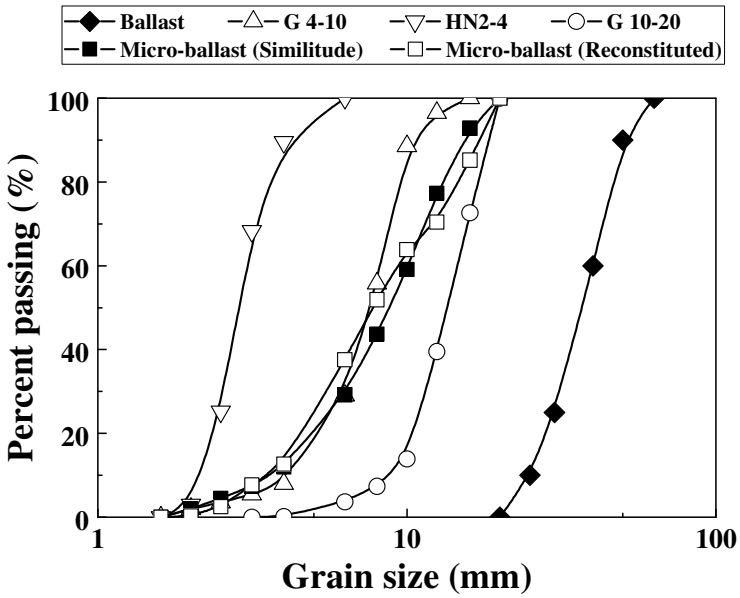

411

Fig. 4. Grain size distribution curves of micro-ballast and ballast (after Wang et al. [10])

412 Fig. 5. Photographs of the samples with various coarse grain contents and compacted at $w_{opt\text{-}f}$
413 = 13.7%

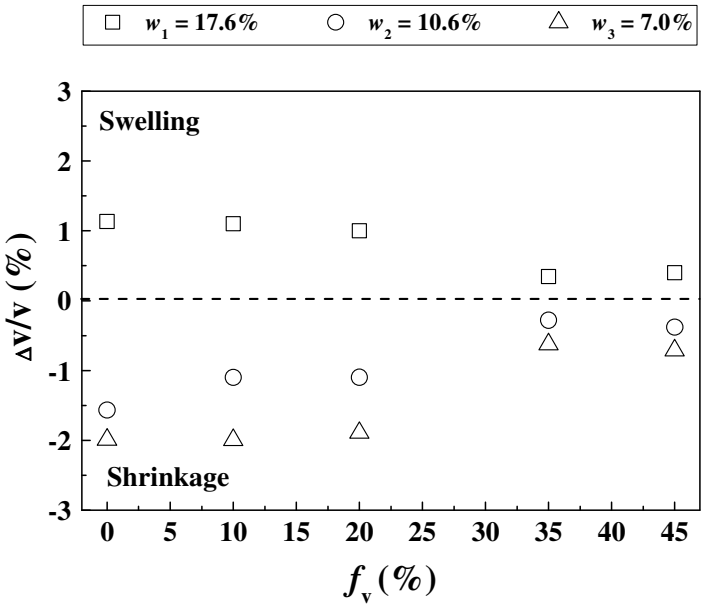

414

415 Fig. 6. Volume change of samples at different f_v values for the three target water contents

416

417

418

419

420

421

422

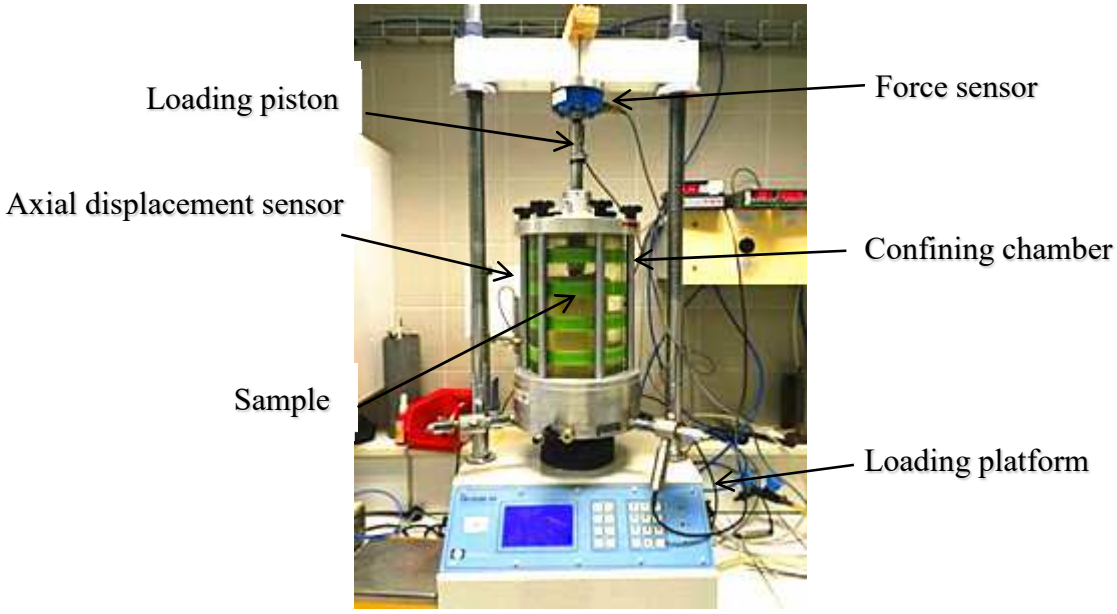

423

424 Fig. 7. Photograph of the monotonic triaxial testing system

425

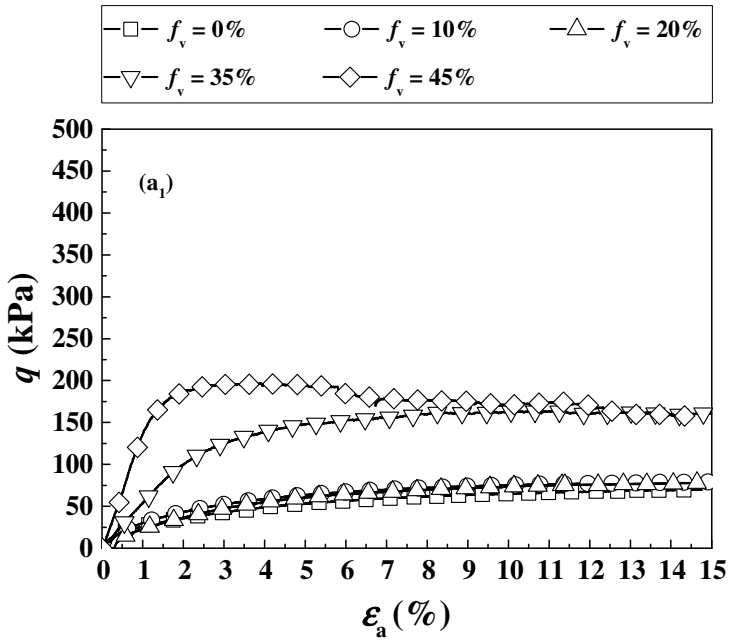

426

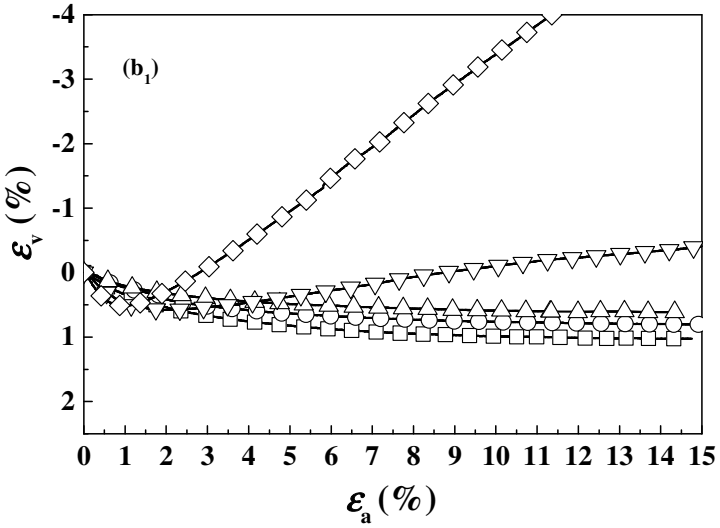

427

428

429

430

431

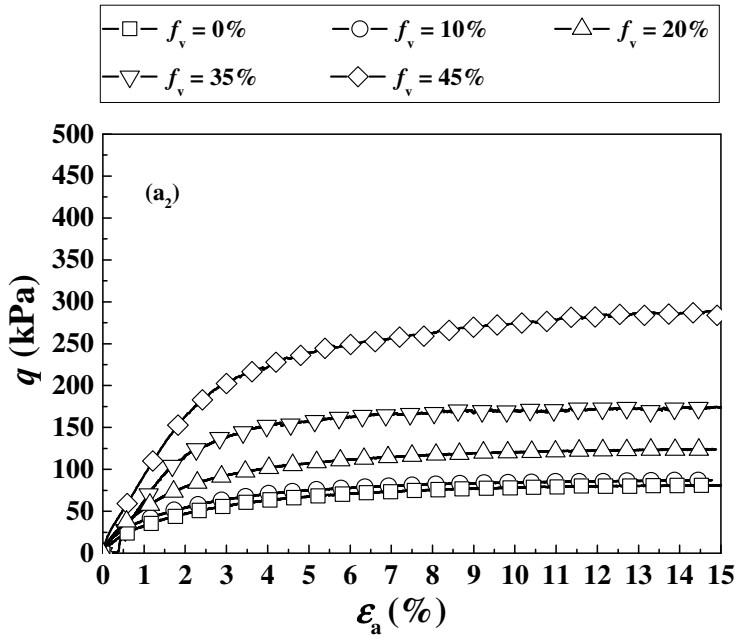

432

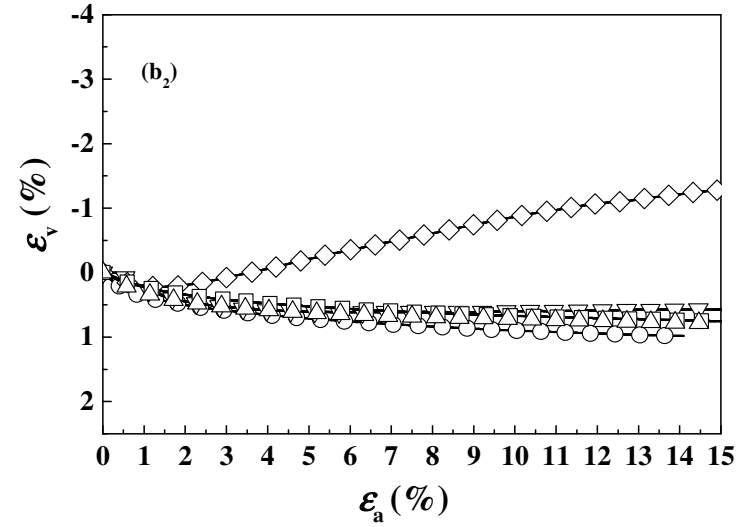

433

434

435

436

437

438

439

440

441

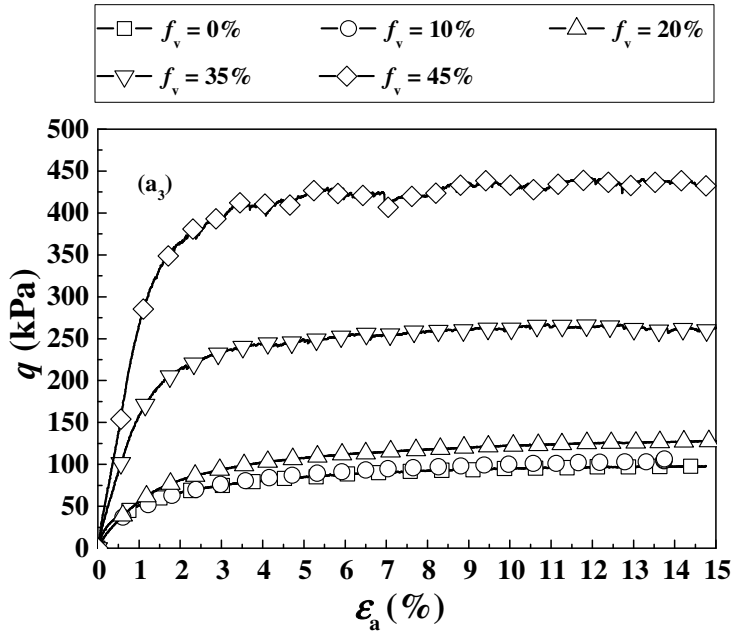

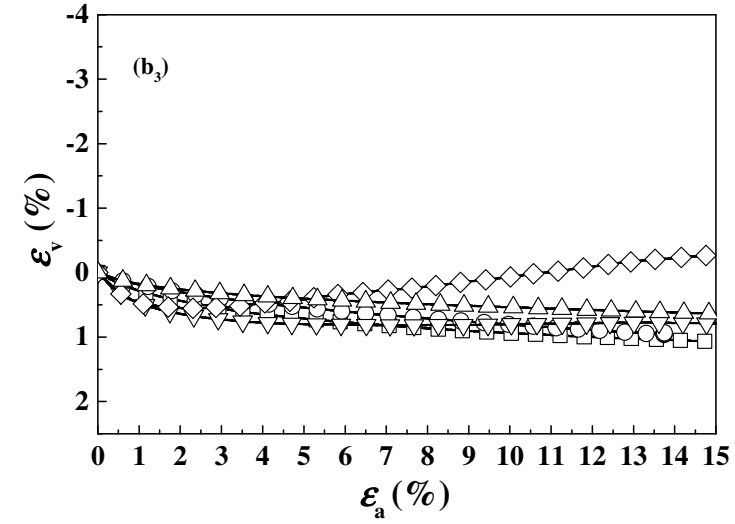

Fig. 8. Results from the tests at w_1=17.6% and different f_v values under:

(a_1) - (b_1) σ_3= 30 kPa; (a_2) - (b_2) σ_3= 60 kPa; (a_3) - (b_3) σ_3= 120 kPa

453

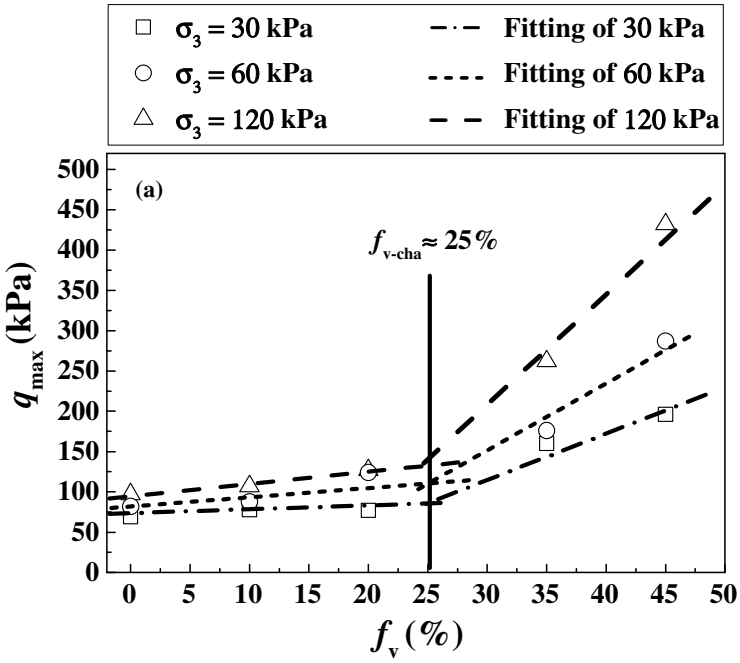

454

455

456

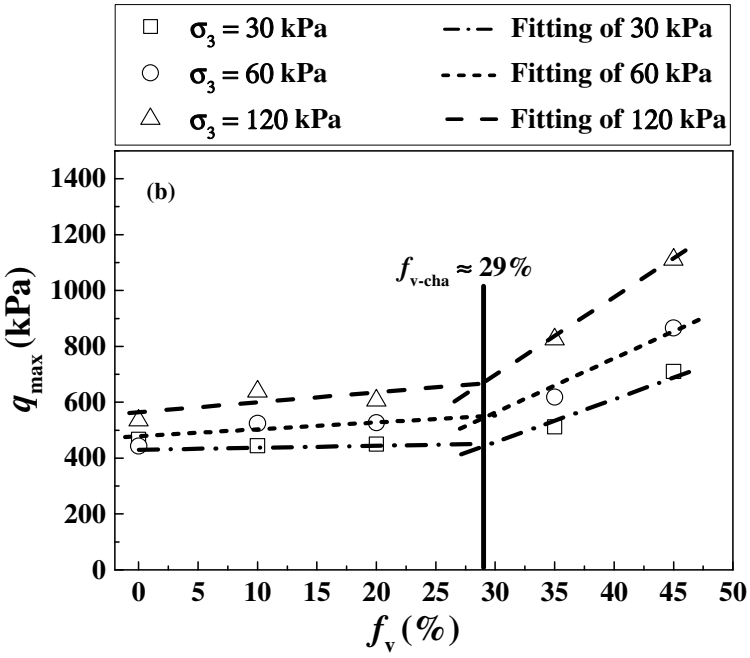

457

458

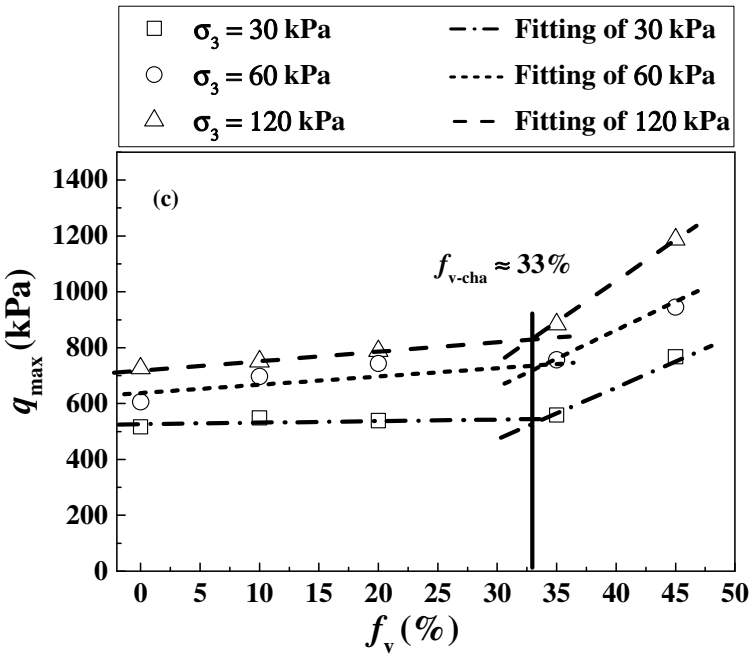

Fig. 9. Variations of peak deviator stress with f_v under different σ_3 values for: (a) $w_1 = 17.6\%$; (b) $w_2 = 10.6\%$; (c) $w_3 = 7.0\%$

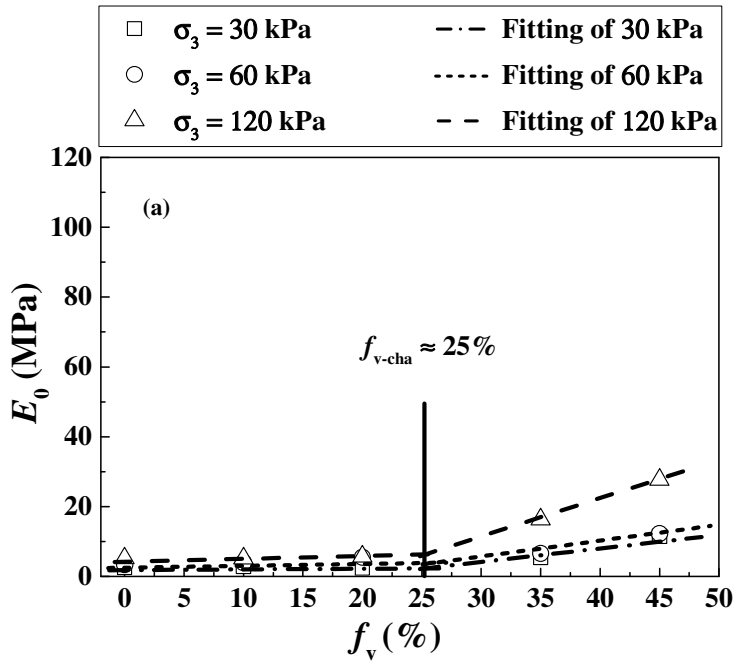

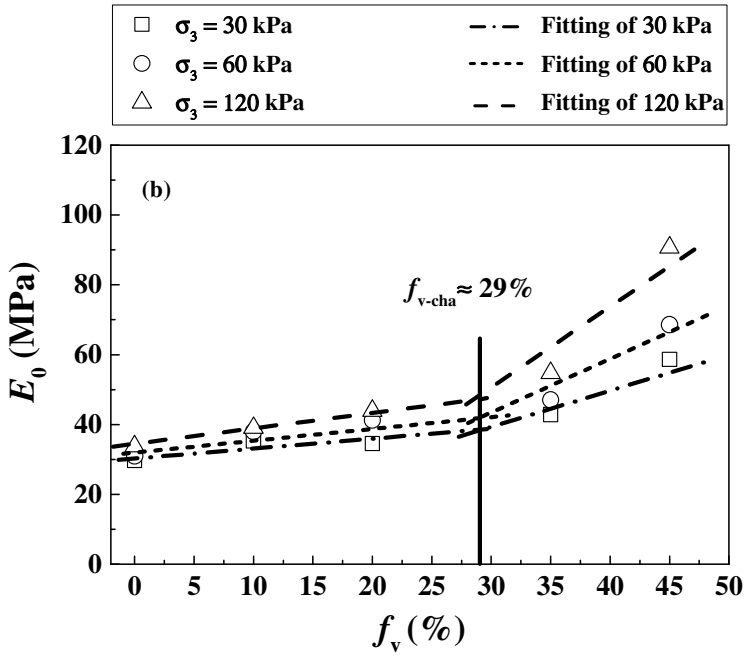

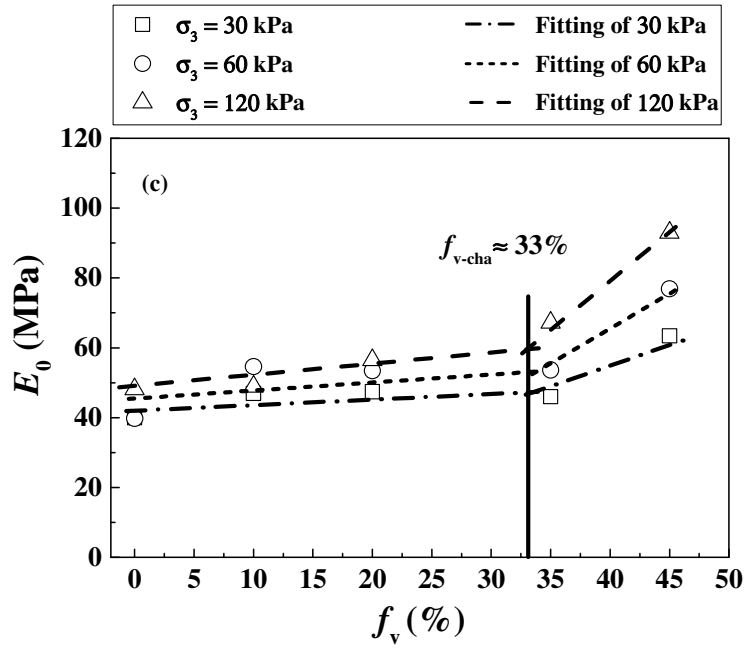

Fig. 10. Variations of initial Young's modulus with f_v under different σ_3 values for: (a) $w_1 = 17.6\%$; (b) $w_2 = 10.6\%$; (c) $w_3 = 7.0\%$

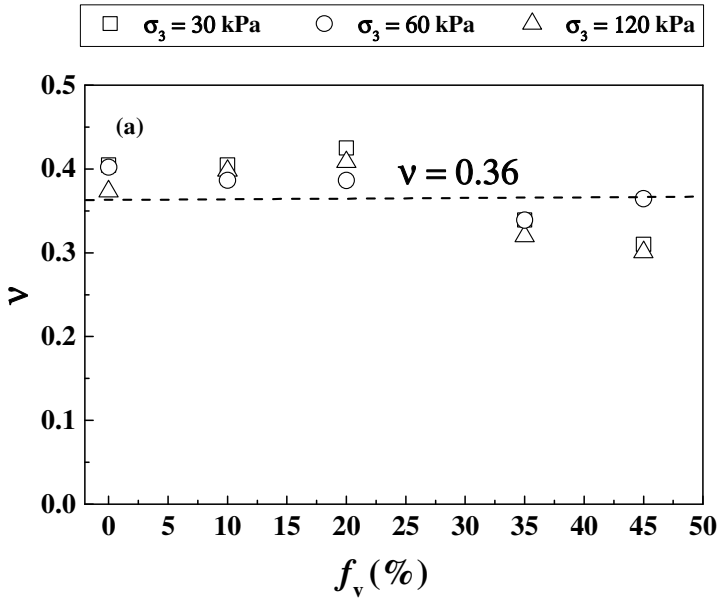
σ3 = 30 kPa
σ3 = 60 kPa
σ3 = 120 kPa
(a)
ν = 0.36
ν
fv (%)

475

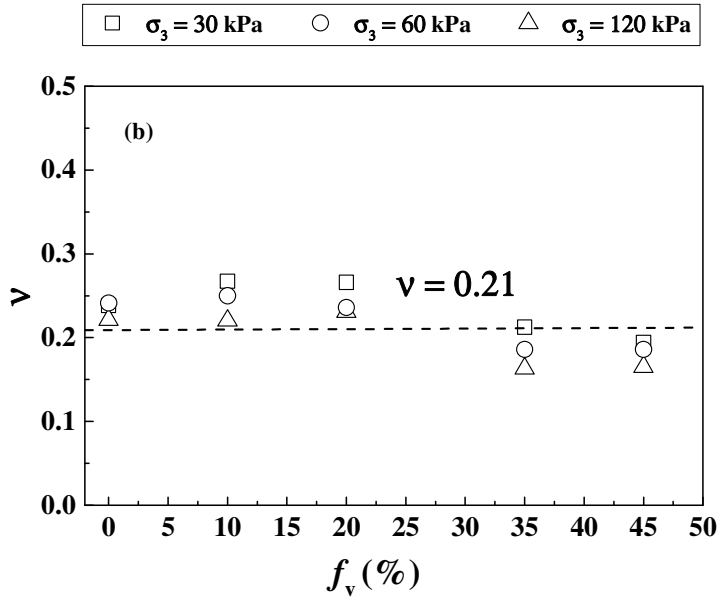
σ3 = 30 kPa
σ3 = 60 kPa
σ3 = 120 kPa
(b)
ν = 0.21
ν
fv (%)

476

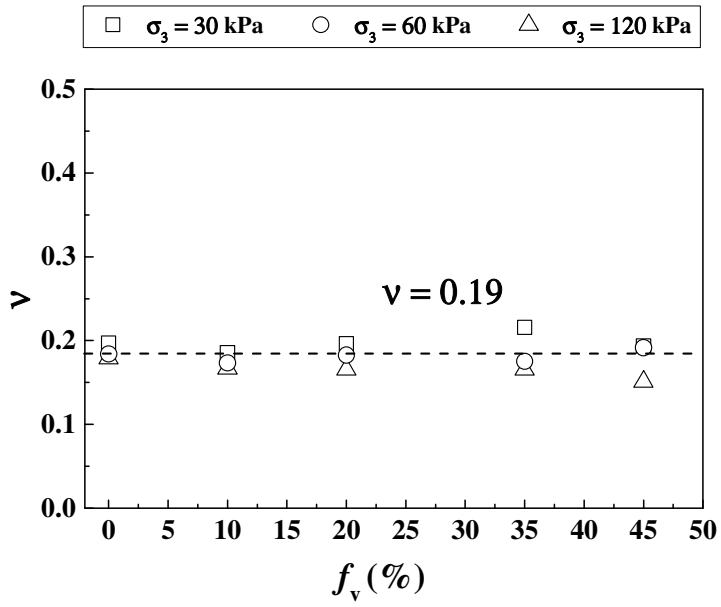

Fig. 11. Variations of Poisson's ratio with f_v under different σ_3 values for: (a) $w_1 = 17.6\%$; (b) $w_2 = 10.6\%$; (c) $w_3 = 7.0\%$

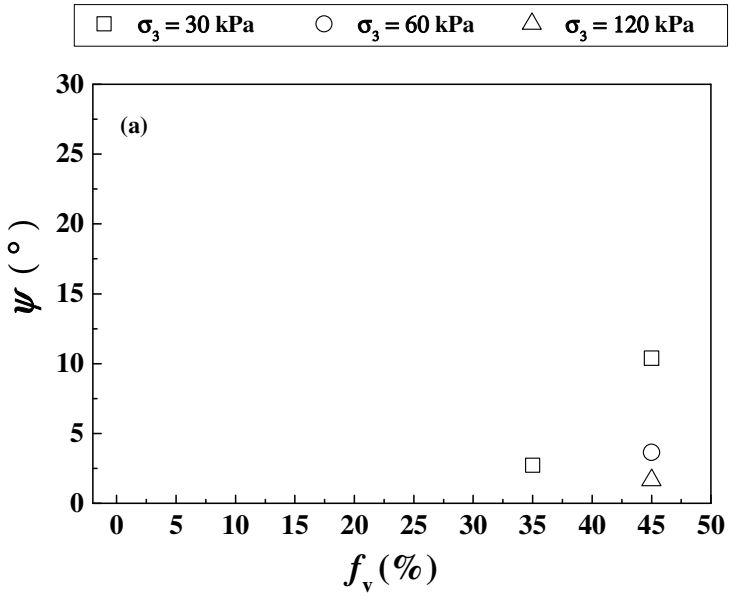

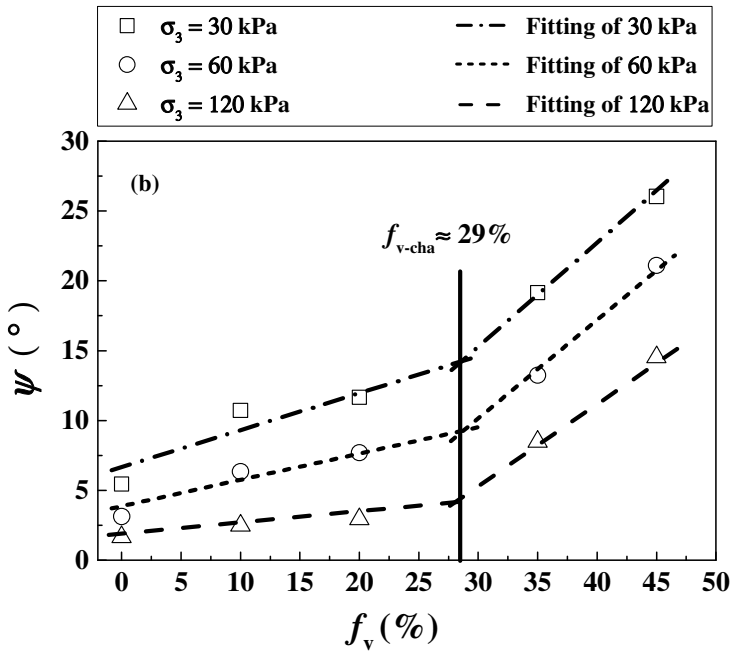

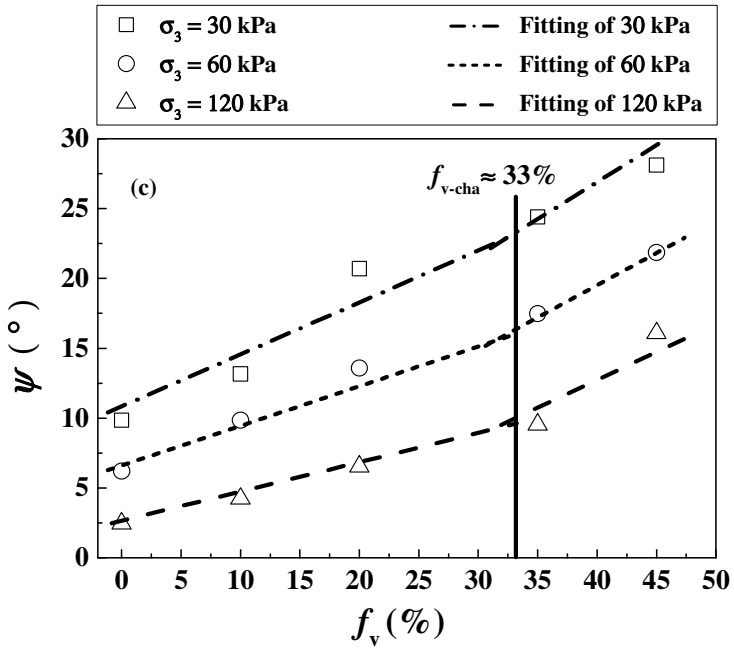

Fig. 12. Variations of dilatancy angle with f_v under different σ_3 values for:

(a) $w_1 = 17.6\%$; (b) $w_2 = 10.6\%$; (c) $w_3 = 7.0\%$

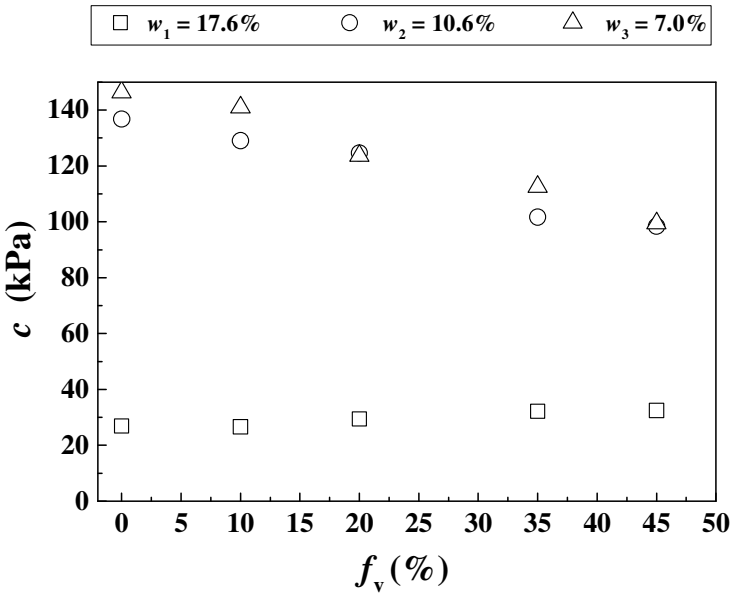

Fig. 13. Variations of cohesion with f_v under different water contents

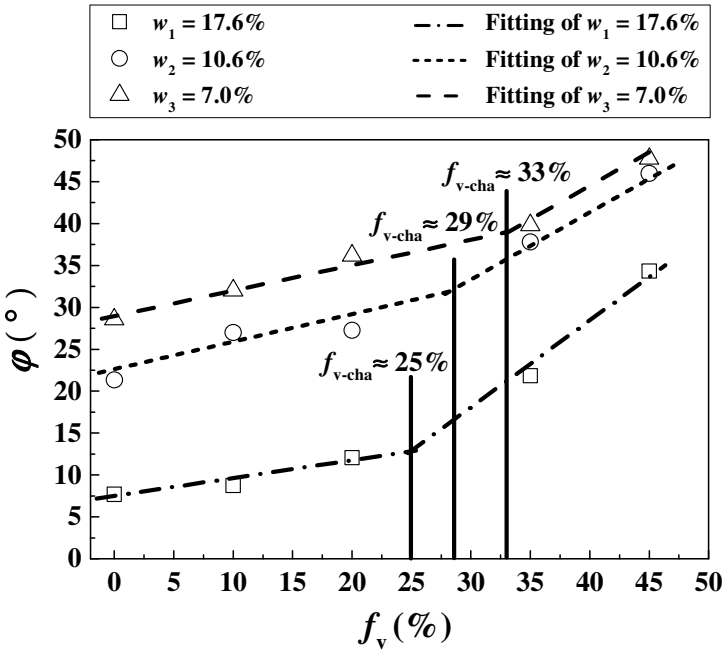

Fig. 14. Variations of friction angle with f_v under different water contents